

Results of recent Pacific-Arctic ice-ocean modeling studies at the Naval Postgraduate School

Jaclyn Clement Kinney and Wieslaw Maslowski

Department of Oceanography, Naval Postgraduate School

Received September 20, 2008

Abstract Summary of results from a high – resolution pan – Arctic ice – ocean model are presented for the northern North Pacific, Bering, Chukchi, and Beaufort seas. The main focus is on the mean circulation, communication from the Gulf of Alaska across the Bering Sea into the western Arctic Ocean and on mesoscale eddy activity within several important ecosystems. Model results from 1979 – 2004 are compared to observations whenever possible. The high spatial model resolution at $1/12^\circ$ (or ~ 9 – km) in the horizontal and 45 levels in the vertical direction allows for representation of eddies with diameters as small as 36 km. However, we believe that upcoming new model integrations at even higher resolution will allow us to resolve even smaller eddies. This is especially important at the highest latitudes where the Rossby radius of deformation is as small as 10 km or less.

Key words numerical modeling, high latitude oceanography, North Pacific, Bering Sea, Chukchi Sea, Beaufort Sea.

1 Introduction

The Naval Postgraduate School (NPS) coupled sea ice-ocean model is a general circulation model (GCM), which has been employed for focused studies of physical ocean and sea ice conditions, as well as interactions between the northern North Pacific and the Arctic Ocean. The model can facilitate further description, intercomparison, and synthesis of multiple ecosystems in the region (Figure 1). The regional model domain includes all of the northern hemisphere sea ice-covered oceans and seas. It contains the sub-Arctic North Pacific (including the Sea of Japan and the Sea of Okhotsk) as well as the North Atlantic (including the Labrador Sea and Gulf of St. Lawrence), the Arctic Ocean, the Canadian Arctic Archipelago (CAA) and the Nordic Seas. The model grid is configured at $1/12^\circ$ (or ~ 9 km) and 45 vertical depth layers with 8 levels in the upper 50 m. This horizontal grid permits calculation of flow through the narrow and / or shallow passages common and critical to sub-polar marginal sea ecosystems.

The ocean model was initialized with climatological, 3-dimensional temperature and salinity fields (Polar Science Center Hydrographic Climatology; PHC) and integrated for almost five decades in a spinup mode. During the spinup we initially used daily-averaged annual climatological atmospheric forcing derived from 1979-1993 reanalysis from the European Centre for Medium-Range Weather Forecasts (ECMWF) for 27 years. We then per-

formed an additional run using repeated 1979-1981 interannual fields for the last 21 years of spinup. This approach is especially important to establishing realistic ocean circulation representative of the time period at the beginning of the actual interannual integration. This final run with realistic daily-averaged ECMWF interannual forcing starts in 1979 and continues through 2004. Results from this integration (26-years) are used for the analyses in this paper. Yukon (and other Arctic) river runoff is included in the model as a virtual freshwater flux at the river mouth. However, in the Gulf of Alaska the freshwater flux from runoff is introduced by restoring the surface ocean level (of 5 m) to climatological (PHC) monthly mean temperature and salinity values over a monthly time scale. Restoring the surface ocean level to climatological temperature and salinity values acts as a correction term to the explicitly calculated fluxes between the ocean and overlying atmosphere or sea ice. Additional details on the model including sea ice, river runoff, and restoring have been provided elsewhere^[1,2].

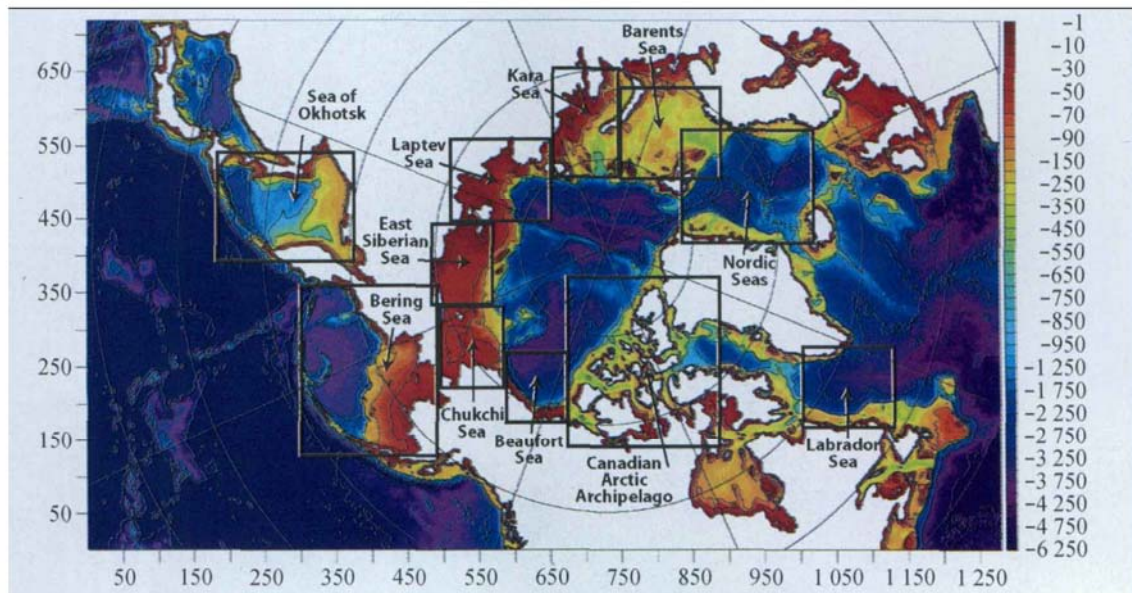


Fig. 1 The NPS model domain (bathymetry in meters; color shading) showing selected multiple ecosystems (black boxes) included in a single model domain.

2 The Northern North Pacific Ocean

Understanding of the mean ocean circulation in the northern North Pacific will provide background and facilitate further investigations of interannual / decadal variability. The upper ocean (0-50m) mean circulation over the 26-year integration (1979-2004) is shown in Figure 2. The prominent Alaskan Stream has a mean volume transport between 34 and 44 Sv, with intensification occurring downstream^[3]. This is similar to observations made near 180°W, which estimated a mean transport of 38.8 Sv^[4,5]. Anticyclonic mesoscale eddies are periodically found propagating along the path of the Alaskan Stream with an average diameter of 168 km and phase speed of $\sim 2.3 \text{ km day}^{-1}$. This is similar to observations by Crawford *et al.* (2000)^[6] who detected the presence of six anticyclonic eddies over a period of seven years with an average diameter of 160 km and a mean phase speed of $\sim 2.5 \text{ km day}^{-1}$. In the model, these eddies do not reduce the strength of the Alaskan Stream, how-

ever there is an off-shore (or southward) shift in the velocity core. Stationary measurement instruments may not be able to detect this shift in position over the slope if their southernmost location does not coincide with the current shift due to an eddy. This may result in recording of a weakened or sometimes reversed flow. The mesoscale eddies also have a strong effect on the volume and property fluxes through the two main eastern and central Aleutian passes^[3]. Large increases in the northward volume, heat, and salt fluxes through Amukta and Amchitka passes occurred during the presence of an eddy in the Alaskan Stream^[3].

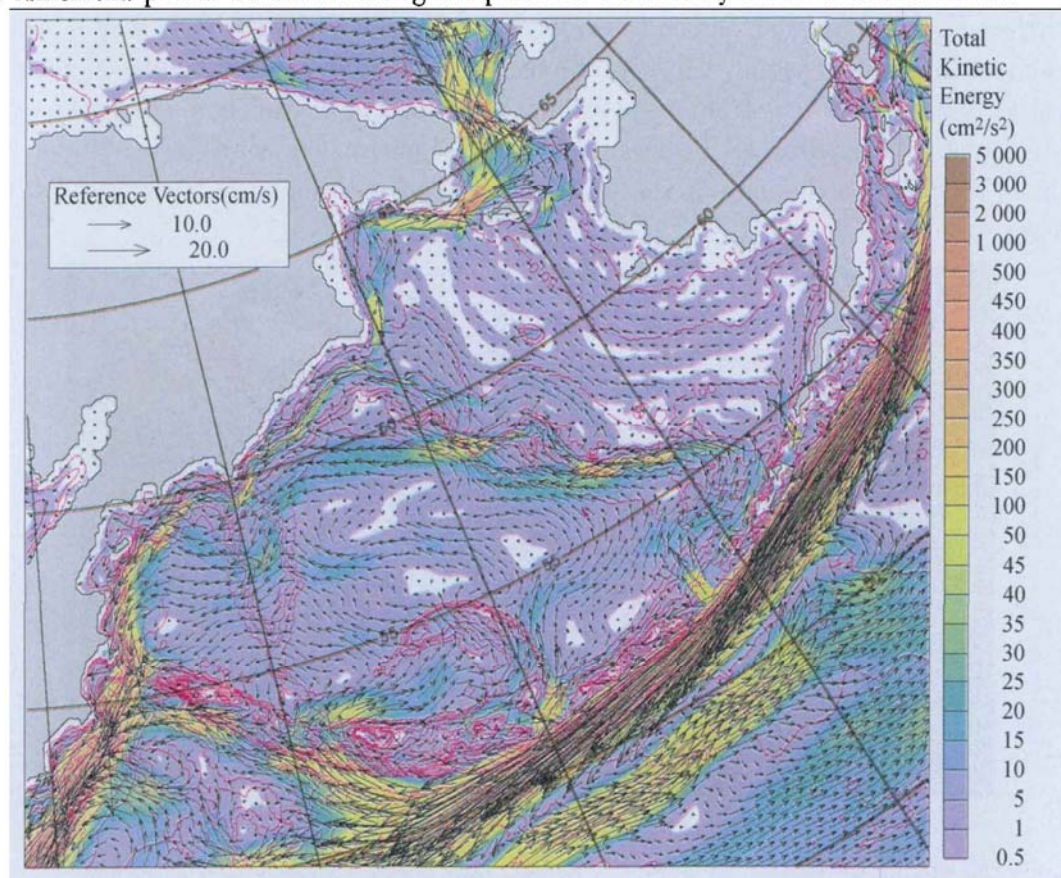


Fig. 2 The 26-year mean (1979-2004) upper 65 m circulation (vectors) and total kinetic energy (shading). Magenta contour lines represent bathymetry (m). Every fourth vector is shown.

3 Bering Sea

Inflow from the Pacific into the Bering Sea via the Aleutian Island passes has already been shown to be affected by mesoscale eddies among other influences (as discussed above). This inflow forms the basis for the Aleutian North Slope Current, while outflow from the Bering Sea occurs primarily via Kamchatka Current near the Siberian coast. We are currently examining the Bering Sea circulation over the deep basin, which is cyclonic in the mean, as shown in Fig. 2. However, animations of model results over time also show frequent eddy activity throughout this area. For instance, at least 14 mesoscale eddies are present in the Bering Sea during June 1987, as shown in Figure 3. Half of these are anticyclonic and the other half are cyclonic. Diameters of these eddies are 120 km and greater and velocities are up to 40 cm/s. Lifetimes of these eddies are typically a few months. The

9-km horizontal resolution of our model allows us to minimally resolve eddies with diameters as small as 36 km, however, we are likely not resolving the smallest eddies. The Bering Sea has a Rossby radius of deformation of $\sim 12\text{--}20$ km according to Chelton *et al.* (1998)^[7].

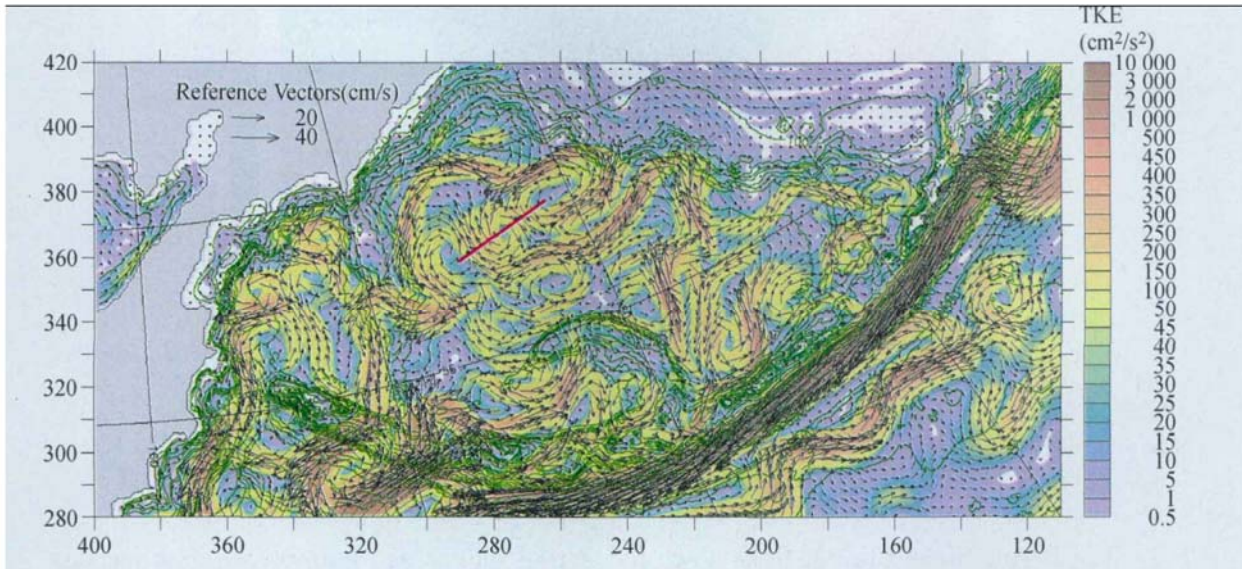


Fig. 3 June 1987 upper 65 m circulation (vectors) and total kinetic energy (shading). Green contour lines represent bathymetry (m). The magenta line indicates the position of a cross section shown in Figure 4. Every third vector is shown.

Eddies are a common feature throughout the deeper part of the Bering Sea. Observations of eddies have been made by Cokelet *et al.* (1996)^[8] and Stabeno and Reed (1993)^[9], among others (e. g. Solomon and Ahlnas 1978^[10]; Kinder *et al.* 1980^[11]; Paluszkiwicz and Niebauer 1984^[12]). Instabilities along the Bering Slope and Kamchatka Currents and interactions with canyons and embayments at the landward edge of these currents and inflows through the Aleutian Island Passes may be responsible for eddy generation^[8]. Stabeno and Reed (1993)^[9] observed several eddies and meanders within the Kamchatka Current and the eastern Bering Sea by utilizing satellite-tracked drifters. Several anticyclonic eddies were observed in the western side of the basin and resulted from the interaction of the Kamchatka Current with topographic features. Stabeno and Reed (1993)^[9] suspect that these features are semi-permanent, since they appeared in drifter trajectories from more than 1 year. Our Fig. 3 shows two anticyclonic eddies associated with the Kamchatka Current during June 1987. A cyclonic eddy (part of a counter-rotating pair) is also present near the Kamchatka Current at that time. Stabeno and Reed (1993)^[9] also observed a large eddy west of Bowers Ridge that had a diameter of ~ 200 km and velocities of 30–40 cm/s. This eddy is similar in size and velocity to those from our model shown in Fig. 3. (Diameters are 120 km and greater, with velocities up to 40 cm/s). Cokelet *et al.* (1996)^[8] also observed a strong anticyclonic eddy here and suggest it may be a recurring feature. A vertical cross-section through one of the anticyclonic eddies is shown in Figure 4. A pool of low-salinity water ($S = 32.4\text{--}32.8$) is carried in the center of the eddy. The pool of water reaches as deep as 50 m. A strong vertical displacement of the isohalines ($> 100\text{m}$) occurs in the presence of the eddy. The displacement is highest on the western side

of the eddy. Northward speeds approach 40 cm/s, while southward speeds are greater than 30 cm/s.

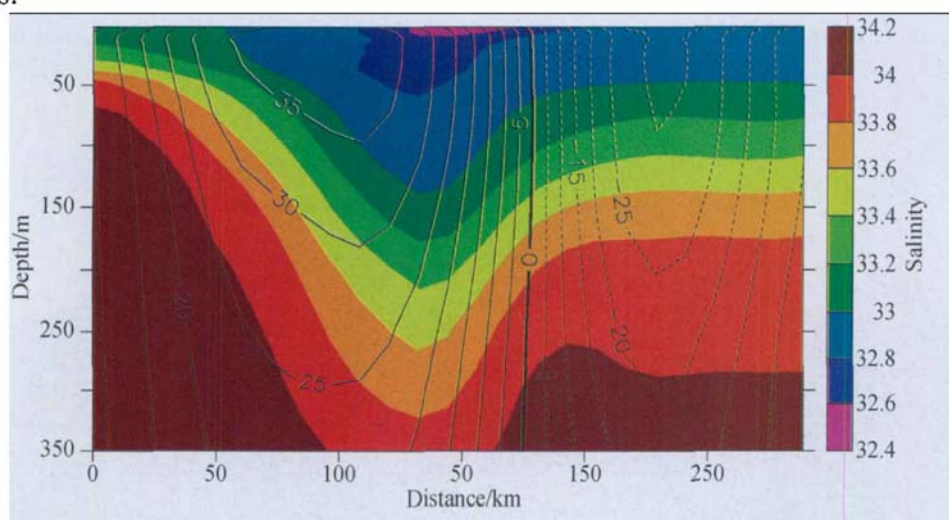


Fig. 4 Salinity (shading) and velocity (contours) across an eddy in the Bering Sea during June 1987. The position of the eddy cross-section is shown as a magenta line in Figure 3.

The Bering Slope Current flows along the Bering shelfbreak, however we find that this current is more a system of eddies rather than a continuous flow. Previously, it was believed that the Bering Slope Current split into two branches (one northward and the other southward) as it neared the coast of Siberia near Cape Navarin. However, our model results show the vast majority of the water follows the bathymetry and turns southward and that very little water from the Bering Slope Current makes the northward turn near the Siberian coast. This is in agreement with a recent schematic circulation proposed by Stabeno *et al.* (1999). An important question for the Bering Sea has been: How does water reach the Bering shelf from the deep basin? First of all, it has been known for quite some time that the Alaska Coastal Current is responsible for carrying the least dense shallow waters from the easternmost Aleutian passes along the coast of Alaska and onto the shelf^[13]. However, for deeper waters, we find that water is periodically pushed onto the shelf along the central and eastern Bering Sea, many times by mesoscale eddy activity. Canyons, such as the Bering and Zhemchug canyons, have larger northward volume fluxes than do other places along the shelfbreak. Water is then accumulated as the mean circulation on the shelf is directed to the northwest. The majority of the northward flow eventually reaching Bering Strait occurs through the narrower, but deeper Anadyr Strait to the west of St. Lawrence Island, with the rest moving northward through Sphanberg Strait east of St. Lawrence Island^[2]. The net volume transport of Pacific-derived water flowing northward through Bering Strait is 0.65 Sv in the mean, which includes a small component of southerly flow. On a seasonal basis, higher values tend to occur in summer and lower values in winter. Observations by Roach *et al.* (1995) and Woodgate *et al.* (2005) provide a similar estimate of 0.80 Sv for the mean northward transport through Bering Strait^[14,15].

4 Chukchi Sea, Beaufort Sea, and Canada Basin

North of Bering Strait, model results show two main branches that are bathymetrically steered and generally flowing northward; one flows between Wrangel Island and Herald Shoal and the other is located east of Herald Shoal. In addition there are two coastal currents: the East Siberian Coastal Current flows northwestward, but reverses periodically, and the Alaskan Coastal Current continues its northward journey along the Alaskan coast. Chukchi Sea water loses a lot of heat to the atmosphere and to sea ice formation as it traverses the shallow shelf. Our model estimates that 72% of the oceanic heat is lost between Bering Strait and the Chukchi shelfbreak, although this calculation is complicated by Atlantic water heat coming from the west, which is not included.

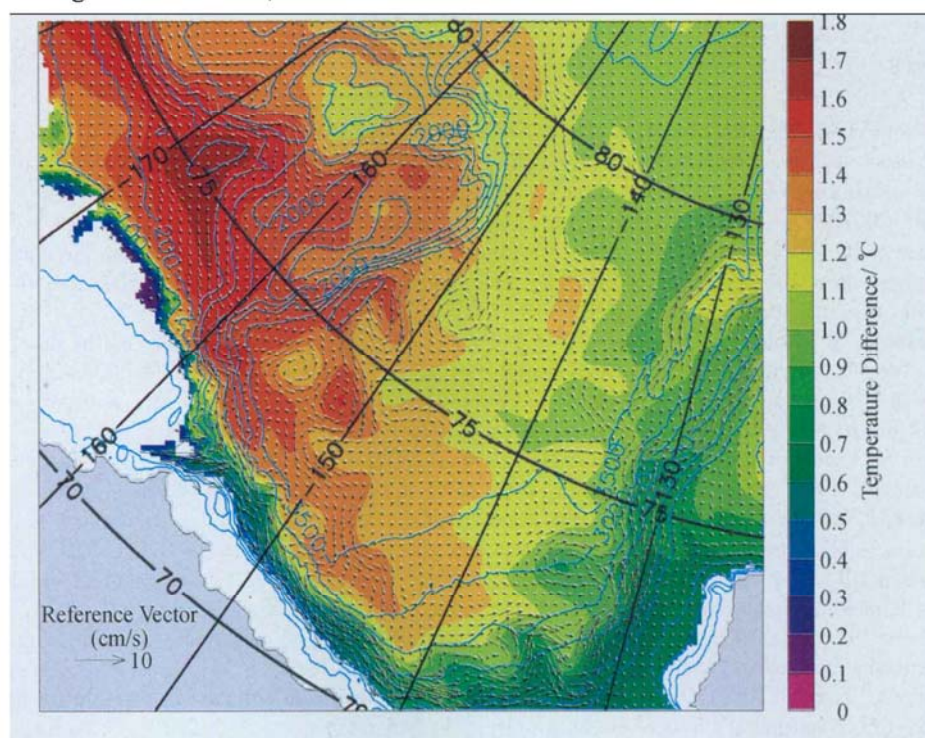


Fig. 5 Depth-averaged (65-120 m) temperature difference ($^{\circ}\text{C}$; temperature minus freezing temperature) and velocity (cm/s) during April 2001. Blue contour lines represent bathymetry (m). Every second vector is shown.

North of $\sim 70^{\circ}\text{N}$, the general circulation begins to head eastward and mixing with East Siberian Sea waters occurs. This eastward flow converges near Barrow Canyon and continues eastward above the Beaufort Sea shelf and slope. To the north of the slope lies the Canada Basin, where observations have identified several subsurface eddies with both cyclonic and anticyclonic rotations^[16,17,18]. Our model results also show the presence of eddies, with an example of an anticyclone shown in Figure 5. The warm core of the anticyclone may affect the overlying sea ice if some of this heat escapes into the mixed layer. We note that the modeled eddies were much larger (typically 80-150 km) than the observed (10-20 km)^[19]. This is due to the limits of our 9-km horizontal resolution and the small radius of deformation at these high latitudes. We believe that our ongoing efforts to increase the horizontal resolution of this model will improve the representation of smaller eddies, which seem to be critical for representing the circulation properly.

Acknowledgements We thank the U. S. National Science Foundation/Shelf-Basin Interactions (SBI) Program for primary support of this research. Additional support has been provided through other National Science Foundation Office of Polar Program (OPP) grants, the U. S. Department of Energy Climate Change Prediction Program (CCPP), and the National Aeronautics and Space Administration Ocean and Ice Program. Computer resources were provided by the Arctic Region Supercomputing Center (ARSC) through the U. S. Department of Defense High Performance Computer Modernization Program (HPCMP). We thank Jia Wang, a guest editor of this volume, and an anonymous reviewer for insightful comments, which improved an earlier version of this manuscript.

References

- [1] Maslowski W, Marble D, Walczowski W, Schauer U, Clement JL, Semtner AJ (2004): On climatological mass, heat, and salt transports through the Barents Sea and Fram Strait from a pan-Arctic coupled ice-ocean model simulation. *Journal of Geophysical Research*, 109: C03032, doi: 10.1029/2001JC001039.
- [2] Clement JL, Maslowski W, Cooper L, Grebeier J, Walczowski W (2005): Ocean circulation and exchanges through the northern Bering Sea - 1979-2001 model results. *Deep Sea Research II*, 52:3509-3540, doi: 10.1016/j.dsr2.2005.09.010.
- [3] Maslowski W, Roman R, Clement Kinney J (2008a): Effects of mesoscale eddies on the flow of the Alaskan Stream. *Journal of Geophysical Research*, 113: C07036, doi:10.1029/2007JC004341.
- [4] Roden GI (1995): Aleutian Basin of the Bering Sea: Thermohaline, oxygen, nutrient, and current structure in July 1993. *Journal of Geophysical Research*, 100:13539 - 13554.
- [5] Chen S, Firing E (2006): Currents in the Aleutian Basin and subarctic North Pacific near the dateline in summer 1993. *J. Geophys. Res.*, 111: C03001, doi:10.1029/2005JC003064, 2006.
- [6] Crawford WR, Cherniawski JY, Forman MGG (2000): Multi-year meanders and eddies in the Alaskan Stream as observed by TOPEX/Poseidon altimeter. *Geophys. Res. Lett.*, 27(7):1025 - 1028.
- [7] Chelton DB, deSzoeke RA, Schlax MG, Naggar KE, Siwertz N (1998): Geographical variability of the first baroclinic Rossby radius of deformation. *J. Phys. Oceano.*, 28:433 - 460.
- [8] Cokelet ED, Schall ML, Dougherty DM (1996): ADCP-referenced geostrophic circulation in the Bering Sea Basin. *Journal of Physical Oceanography*, 26: 1113 - 1128.
- [9] Stabeno PJ, Reed RK (1993): Circulation in the Bering Sea Basin observed by satellite-tracked drifters: 1986-1993. *Journal of Physical Oceanography*, 24: 848 - 854.
- [10] Solomon H, Ahlnas K (1978): Eddies in the Kamchatka Current. *Deep-Sea Research*, 25:403 - 410.
- [11] Kinder TH, Schumacher JD, Hansen DV (1980): Observations of a baroclinic eddy: An example of mesoscale variability in the Bering Sea. *Journal of Physical Oceanography*, 10:1228 - 1245.
- [12] Paluszkievicz, T, Niebauer HJ (1984): Satellite observations of circulation in the eastern Bering Sea. *Journal of Geophysical Research*, 89:3663 - 3678.
- [13] Schumacher JD, Pearson CA, Overland JE (1982): On exchange of water between the Gulf of Alaska and the Bering Sea through Unimak Pass. *Journal of Geophysical Research*, 87:5785 - 5795.
- [14] Roach AT, Aagaard K, Pease CH, Salo SA, Weingartner T, Pavlov V, Kulakov M (1995): Direct measurements of transport and water properties through the Bering Strait. *Journal of Geophysical Research*, 100:18443 - 18457.
- [15] Woodgate RA, Aagaard K, Weingartner T (2005): Monthly temperature, salinity, and transport variability of the Bering Strait throughflow. *Geophysical Research Letters*, 32(4) L04601, doi:10.1029/2004GL021880.
- [16] Manley TO, Hunkins J (1985): Mesoscale eddies of the Arctic Ocean. *J. Geophys. Res.*, 90(C3): 4911 - 4930.
- [17] D'Asaro EA (1988): Observations of small eddies in the Beaufort Sea. *J. Geophys. Res.*, 93(C6): 6669 - 6684.
- [18] Plueddemann AJ, Krishfield R, Takizawa T, Hatakeyama K, Honjo S (1998): Upper ocean velocities in the Beaufort Gyre. *Geophys. Res. Lett.*, 25(2):183 - 186.
- [19] Maslowski W, Clement Kinney J, Marble DC, Jakacki J (2008b): Towards eddy-resolving models of the Arctic Ocean. In: *Ocean Modeling in an Eddying Regime*, MW Hecht and H Hasumi, eds. *Geophysical Monograph Series*, 177: 350.